



# Integrated Biostratigraphy, Depositional Setting and Geochemical Analyses for Petroleum Potential Evaluation of the Lower Cretaceous (Barremian – Albian) Strata of the Koppeh-Dagh Basin, Northeastern Iran

Sharifi MOHAMMAD<sup>1</sup>, Foroughi FARIBA<sup>1</sup>, Ghasemi-Nejad EBRAHIM<sup>1,\*</sup>, Shekarifard ALI<sup>2</sup>, Yazdi-Moghadam MOHSEN<sup>3</sup> and Sarfi MEHDI<sup>4</sup>

<sup>1</sup> Department of Geology, Faculty of Sciences, University of Tehran, Tehran, Iran

<sup>2</sup> School of Chemical Engineering, College of Engineering, University of Tehran, Tehran, Iran

<sup>3</sup> Exploration Directorate of the National Iranian Oil Company, Tehran, Iran

<sup>4</sup> School of Earth Sciences, Damghan University, Damghan, Iran

**Abstract:** The lower Cretaceous rock units of the Koppeh-Dagh Basin of northeastern Iran were investigated here in terms of biostratigraphy, depositional setting and geochemical analyses to find out if they, like other parts of the world, are rich in petroleum. For this purpose, a stratigraphic framework is established using calcareous nannofossil and palynological elements. A nannoplankton zonation based on which subzones of the zones CC7 – CC8 of Sissingh (1977) and their equivalent NC6 – NC8 of Roth (1978) was established indicating a Late Barremian–Albian age. Palynological assemblages led us to establish the local palynozone of *Odontochitina operculata*. A dominantly marginal basin to a transitional zone between shelf and basin under a dysoxic–anoxic condition with low to moderate sedimentation rates coincided with a gradual sea level rise was introduced as the environment of deposition for the strata via interpretation of the palynological parameters and quantitative palynology. The obtained data from Rock-Eval pyrolysis in compilation with palynofacies analysis reveals that the studied succession contains mainly gas-prone type III kerogen. The Spore Coloration Index (SCI) alongside with the Rock-Eval pyrolysis results (low values of HI and TOC) proves that these rock units locally produced natural gas during the time under consideration.

**Key words:** Koppeh-Dagh, Lower Cretaceous, Biostratigraphy, Palaeoenvironment, Rock-Eval pyrolysis

Citation: Mohammad et al., 2019. Integrated Biostratigraphy, Depositional Setting and Geochemical Analyses for Petroleum Potential Evaluation of the Lower Cretaceous (Barremian – Albian) Strata of the Koppeh-Dagh Basin, Northeastern Iran. Acta Geologica Sinica (English Edition), 93(6): 1885–1899. DOI: 10.1111/1755-6724.13823

## 1 Introduction

Because of some important events that took place during the Cretaceous, this period is important in terms of geological and palaeontological studies. As the last and longest segment of the Mesozoic Era, the Cretaceous period is known for its domination of warm and humid climates, massive rifts and huge volcanic eruptions breaking giant supercontinents into smaller landmasses, rising sea levels and spreading low-oxygen conditions in oceanic basins (Steuber et al., 2005; Tejada et al., 2009; Keller et al., 2011). The simultaneous occurrence of these events led to the deposition of the largest amount of source rocks in the Cretaceous basins, especially in the Aptian-Turonian interval (Ulmishek and Klemme, 1990). These source rocks mainly formed from shales and marls with kerogen types II and III that generated Upper Cretaceous–Cenozoic petroleum (oil and gas) accumulations in the basins (Ulmishek and Klemme,

1990). The Koppeh-Dagh Basin, which is considered a part of the northern Tethyan realm (Glennie, 2000) is located between Iran, Afghanistan and Turkmenistan (Fig. 1a) and is known for its high hydrocarbon potential and gas reservoirs (Kavoosi et al., 2010). The Sarcheshmeh and Sanganeh formations being studied here are shaly marine sequences of early Cretaceous age deposited in this basin. Both formations are rich in marine phytoplanktons, dinoflagellate cysts and coccolithophores. Dinoflagellates play a key role among the Cretaceous Tethyan microflora and therefore, are studied widely for their stratigraphical and environmental values in petroleum potential interpretations (Oosting et al., 2006; Quattrocchio et al., 2006; Backhouse, 2006; Ghasemi-Nejad et al., 2009; Radmacher et al., 2014; Gard et al., 2016; Tahoun et al., 2018). As this study is focused on the Iranian part of the Koppeh-Dagh Basin, its main objectives are (a) establishing an accurate stratigraphic framework via dinoflagellate cysts and calcareous nannofossils in order to date the two formations precisely, (b) reconstructing the palaeoenvironment of these strata and its dominant

\* Corresponding author. E-mail: eghasemi@khayam.ut.ac.ir

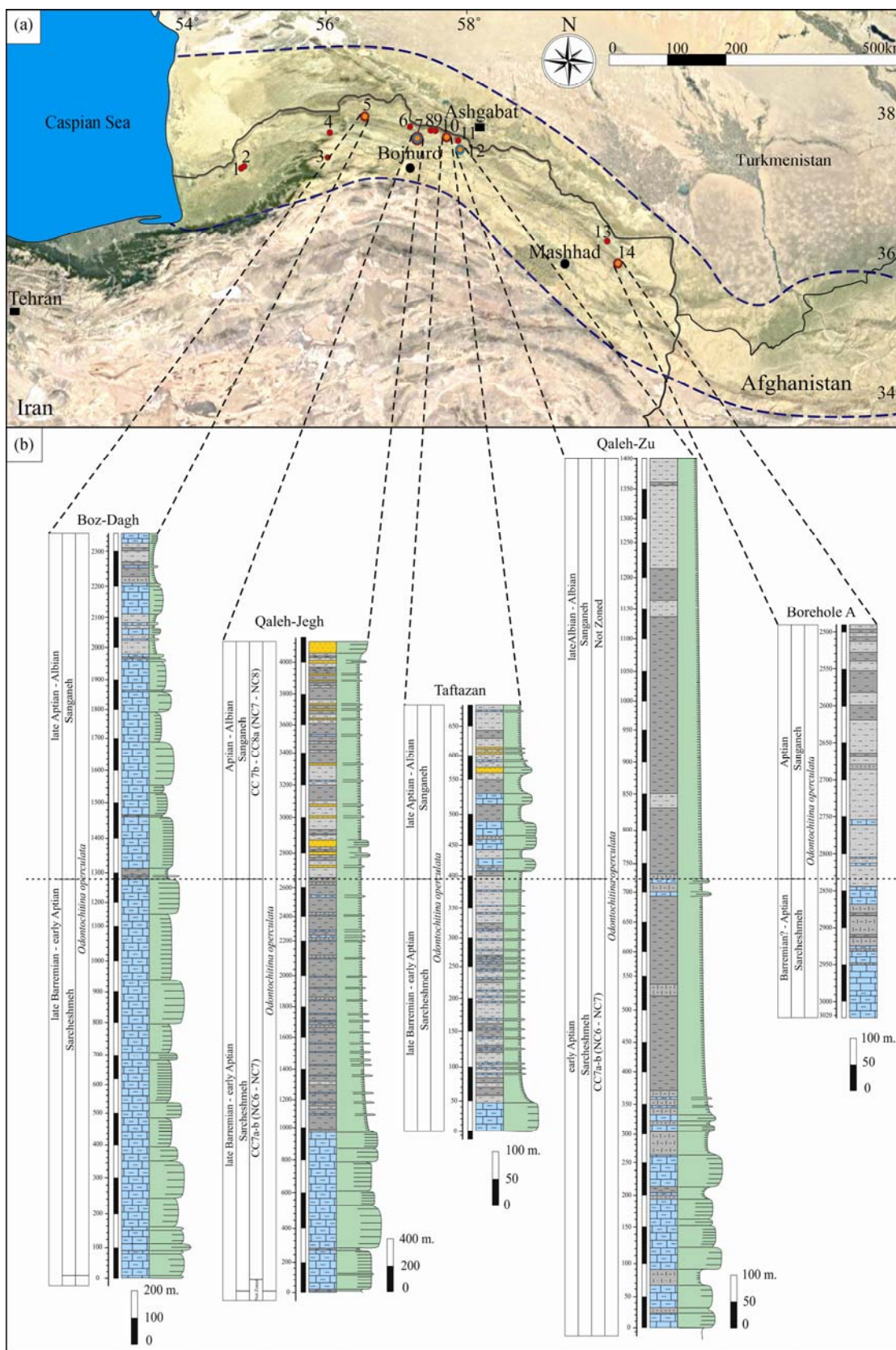


Fig. 1. (a) Location map of the Koppeh-Dagh Basin and the sections studied; orange circles; sections sampled and studied for palynological contents; blue circles; sections sampled and studied for calcareous nannofossils contents; red circles; section for which Rock-Eval pyrolysis data were available and used. (b) Lithostratigraphic logs of the sections sampled and studied (for details of the logs see Table 1).

condition in order to determine the possibility of having favorable condition for hydrocarbon source rocks deposition, and (c) evaluating these fine-grained rock units in order to assess their petroleum potential and find out whether they could have acted as source rocks.

## 2 Geological Setting

During the Cretaceous, the warmer Tethyan seaway separated the northern from the southern Boreal realms and endured different episodes of sea level rising. Sometimes these sea level rises were synchronous with minimal temperature differences between the poles and the equator (e.g. Norris et al., 2002; Huber et al., 2002; Bice et al., 2006; Dumitrescu et al., 2006; Bornemann et al., 2008) that led to extension of oceanic anoxic events (OAEs) in the bottom waters of the Tethyan realm. The Koppeh-Dagh Basin is an inverted structure (Garzanti and Gaetani, 2002; Allen et al., 2003) in which the relatively continuous sedimentation during Jurassic to Eocene resulted in deposition of the thickest Cretaceous deposits in Iran (Afshar-Harb, 1994). A large-scale sea level rise occurred in Early Cretaceous formed a transgressive sedimentary mega-sequence that includes four formations. The succession begun with the terrigenous Shurijeh Formation of the Neocomian age that turns to the shallow shelfal carbonates of the Tirgan Formation with an age of Barremian–Early Aptian (Afshar-Harb, 1994). These carbonates are in turn succeeded by the relatively deep marine strata of the Sarcheshmeh and Sanganeh formations (Robert et al., 2014).

## 3 Material and Methods

A total of 529 rock samples from the two formations under study were collected from four outcrop sections and an exploratory well for palynological studies (see table 1 and figure 1b for details). Palynological slides were prepared following the conventional maceration procedure of Traverse (2007). The slides were studied under a light microscope for their palynological contents and some statistical practices are implemented to calculate percentages of the three main types of kerogens, including

**Table 1 Summary of the stratigraphic sections' co-ordinates and sample characteristics in the present study (Sr. stands for Sarcheshmeh and Sn. For Sanganeh Formation)**

| ions       | co-ordinates     | Fm. | Thickness (m) | Palynology | Nannofossils |
|------------|------------------|-----|---------------|------------|--------------|
| Qaleh-Jegh | E 57 ° 15' 51.5" | Sr. | 2660          | 210        | 221          |
|            | N 37 ° 47' 38"   | Sn. | 1400          | 51         | 96           |
| Qaleh-Zu   | E 57 ° 48' 07"   | Sr. | 713           | 36         | 86           |
|            | N 37 ° 29' 39"   | Sn. | 638.5         | 21         | 53           |
| Boz-Dagh   | E 56 ° 41' 0.87" | Sr. | 1272.5        | 43         | 0            |
|            | N 37 ° 50' 41"   | Sn. | 1091          | 39         | 0            |
| Taftazan   | E 57 ° 48' 16.3" | Sr. | 396           | 15         | 0            |
|            | N 37 ° 45' 58.3" | Sn. | 298           | 19         | 0            |
| Borehole A | -                | Sr. | 177           | 48         | 0            |
|            | -                | Sn. | 348           | 47         | 0            |
| Total      |                  |     |               | 529        | 456          |

Note: For confidential reasons of the NIOC, the real name and co-ordinates of the studied well aren't recorded here and the subsurface section is renamed as borehole A.

amorphous organic matters (AOMs), terrestrial elements (phytoclasts) and marine palynomorphs in each sample for detailed palynofacies and palaeoecological investigations. Also to establish a high resolution stratigraphic framework, smear-slides are prepared from 456 samples using gravity settling method (Bown, 1998) and studied for their calcareous nannofossils content. Calcareous nannofossil preservation was evaluated qualitatively using visual criteria concerning the degree of etching and overgrowth (Watkins, 2007). The Tethyan realm fundamental nannozoneations based on CC biozonation scheme (Sissingh, 1977) modified by Perch-Nielsen (1985) and NC biozonation scheme (Roth, 1978) with subdivisions after Bralower (1987) and Bralower et al., (1993) were applied. For evaluation of the petroleum potential and generation Rock-Eval data of 63 samples gathered from eleven stratigraphic sections and three wells (for details see Fig. 1a) available at the NIOC were included and used for interpretations. The data were gained using Rock-Eval 6 at the Research Institute of the Petroleum Industry of Iran. In this method that is well-documented in literature (e.g., Espitalié et al., 1977; Tissot and Welte, 1984; Peters et al., 2005), carbon compounds are released consecutively from rock samples by steady heating of the samples from 300 to 650 °C at a rate of 25 °C per minute in an inert atmosphere (helium or nitrogen). The obtained data are summarized in Table 2. Eventually, a combination of palynofacies analysis and geochemical pyrolysis are used for evaluation of rock units in terms of prevailed palaeoenvironmental conditions and petroleum potential and generation.

## 4 Results and Discussion

### 4.1 Stratigraphic framework

#### 4.1.1 Marine palynology and palynostratigraphy

Dinoflagellates increased in number and diversity from the Neocomian to Albian. This additive trend is considered as a reflection to sea level rising and transgressions (Stover et al., 1996). The present study, disclosed dominance of dinoflagellate cysts in both studied formations however, terrestrial palynomorphs (spore and pollen grains) and acritarchs (*Michrhystridium* spp. and *Pterospermella* spp.) were also present. The assemblages recovered are generally dominant by such genera as: *Achomosphaera*, *Circulodinium*, *Cribroperidinium*, *Hystrichodinium*, *Kiokansium*, *Odontochitina*, *Oligosphaeridium* and *Spiniferites* (Fig. 2) alike other parts of the Tethyan reported by many researchers (e.g. Torricelli, 2000; Helby et al., 2004). Based on the presence of such forms as *Achomosphaera neptuni*, *Cerbia tabulata*, *Florentinia mantelli*, *Hystrichosphaerina schindewolfii*, *Kleithriasphaeridium cooksoniae*, *Kleithriasphaeridium eoniodes*, *Muderongia parjata*, *Pseudoceratium anaphrissum*, an age of late Barremian to Aptian is assigned to the Sarcheshmeh Formation. An age of Aptian–Albian is also suggested for the overlying Sanganeh Formation based on the presence of *Achomosphaera ramulifera*, *Cerbia tabulata*, *Chatangiella* sp., *Diconodinium* sp., *Hystrichosphaerina schindewolfii*, *Isabelidinium* sp., and *Pseudoceratium*

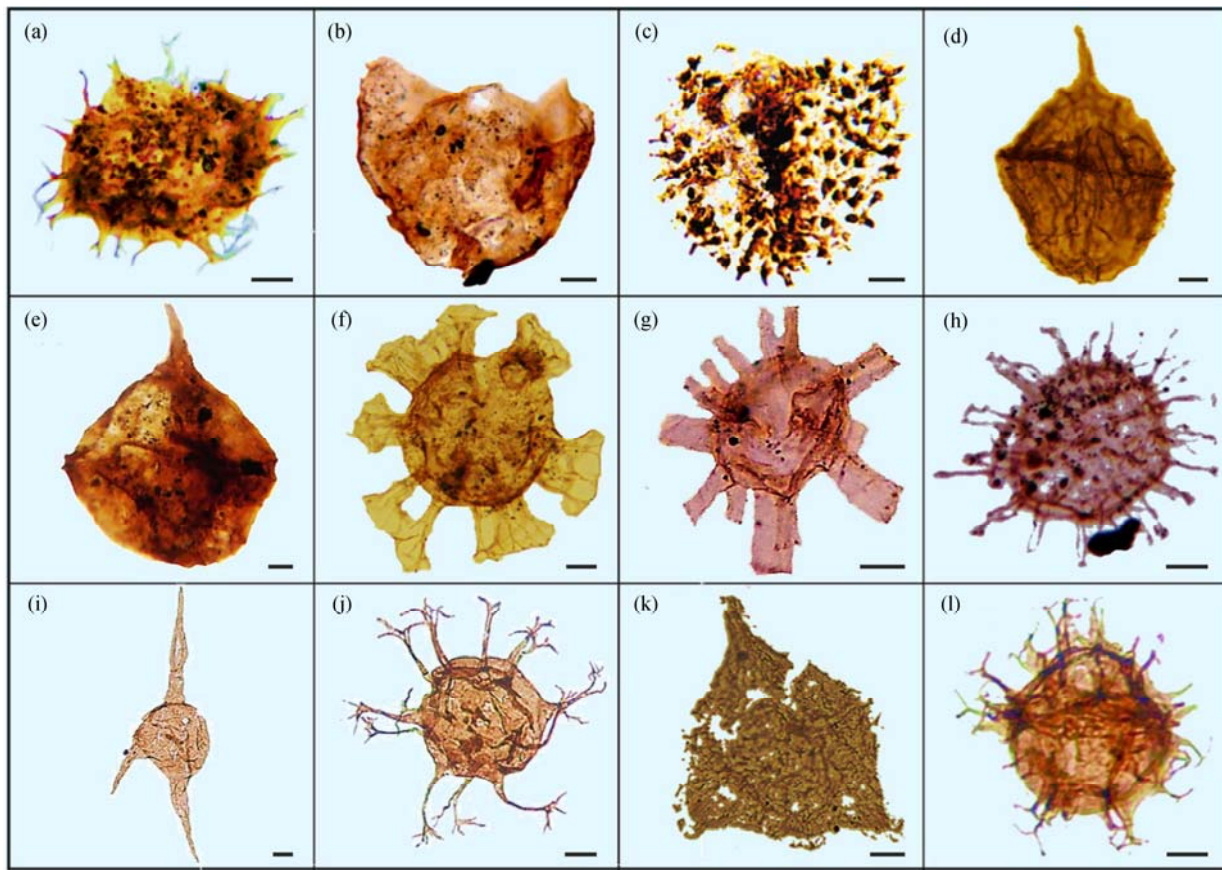


Fig. 2. Some of the recorded dinocysts from the Sarcheshmeh (=Sr.) and Sanghaneh (=Sn.) formations. Scale bars for all pictures represent 10  $\mu$ m.

(a) *Achomospaera neptuni*, Taftazan section, Sample No. MAL 6889, Sr. Fm.; (b) *Cerbia tabulata*, Bozdagh section, Sample No. HZ 4132, Sn. Fm.; (c) *Circulodinium distinctum*, Borehole A, Sample No. 2780, Sn. Fm.; (d) *Cribroperidinium edwardsii*, Qaleh-Zu section, Sample No. MEMO 203, Sr. Fm.; (e) *Cribroperidinium orthoceras*, Taftazan section, Sample No. MOTA 1691, Sn. Fm.; (f) *Hystrichosphaerina schindewolfii*, Qaleh-Zu section, Sample No. MEMO 222, Sr. Fm.; (g) *Kleithrisphaeridium cooksoniae*, Bozdagh section, Sample No. HZ 3939, Sr. Fm.; (h) *Kiokansium polyopes*, Bozdagh section, Sample No. HZ 4100, Sn. Fm.; (i) *Odontochitina operculata*, Qaleh-Jegh section, Sample No. MAL 4825, Sr. Fm.; (j) *Oligosphaeridium complex*, Qaleh-Jegh section, Sample No. MAL 4673, Sr. Fm.; (k) *Pseudoceratium anaphrissum*, Qaleh-Zu section, Sample No. MEMO 222, Sr. Fm.; (l) *Spiniferites ramosus*, Qaleh-Jegh section, Sample No. MAL 4673, Sr. Fm.

#### *anaphrissum*.

The two studied formations are similar in terms of dinoflagellate cyst assemblages and even lithology, making almost impossible to differentiate the dinocyst events recorded for the late Barremian to Albian of many parts of the Tethys (Morgan et al., 2002; Helby et al., 2004; Partridge, 2006). However, the assemblages are in a close similarity and reasonable accordance with the *Odontochitina operculata* Opper Zone of Helby et al. (2004), which has already been reported from the Koppeh-Dagh Basin (Sharifi et al., 2018). The zone may cover as long back as the late Barremian and extend up into the Albian in this area.

#### 4.1.2 Calcareous nannofossils and nannostratigraphy

Calcareous nannoplanktons have largely been used for biostratigraphy of the lower Cretaceous and in hydrocarbon exploration projects (Bown, 1998; Tremolada et al., 2006; Foroughi et al., 2017) mainly due to their small size and preservation in small cutting chips. More recently they have been used for detection of major

palaeoceanographic events such as OAEs as nannoconid crisis precedes the Early Aptian oceanic anoxic event 1a (Bellanca et al., 2002; Erba, 2004; Erba et al., 2010). During this crisis, dinoflagellates and cyanobacteria were dominant phytoplanktons in the oceans (Torricelli, 2000; van Bruegel et al., 2007), though oligotrophic nannoconoids disappeared and coccoliths and peculiar nannoliths (e.g. *Assipetra* and *Rucinolithus*) were abundant forms in the nannoplankton assemblages (Tremolada and Erba, 2002; Herrle and Mutterlose, 2003; Erba and Tremolada, 2004). In order to enhance the accuracy of the age reconstructed framework, nannofossils were studied from Qaleh-Jegh and Qaleh-Zu sections (Fig. 3). At the Qaleh-Jegh stratigraphic section, the basal part of the Sarcheshmeh Formation with a thickness of 88 meters, revealed a barren zone but, according to the recorded forms from the upper parts, the CC7a and partial parts of CC7b nannozones of Sissingh (1977) and NC6 and partial parts of NC7 nannozones of Roth (1978) schemes are constrained based upon which an age of late Barremian-early Aptian can be assigned to the formation.

**Table 2 Rock-Eval data for the pyrolyzed samples (section numbers refer to figure 1a)**

| Sections           | Fm.         | Sample ID  | Petroleum potential (quantity) |      |      |       | S3   | Kerogen type (quality) |        |       | S1/TOC | Thermal maturity |      |
|--------------------|-------------|------------|--------------------------------|------|------|-------|------|------------------------|--------|-------|--------|------------------|------|
|                    |             |            | TOC                            | S1   | S2   | S1+S2 |      | HI                     | OI     | S2/S3 |        | Tmax             | PI   |
| 1                  |             | QT-1 4957  | 5.32                           | 0.89 | 29   | 29.89 | 0.95 | 544.2                  | 17.86  | 30.53 | 0.17   | 421              | 0.03 |
|                    |             | QT-1 8901  | 3.43                           | 0.63 | 17.4 | 18    | 0.83 | 506                    | 24.2   | 20.96 | 0.18   | 422              | 0.03 |
|                    |             | QT-1 9868  | 1.96                           | 0.18 | 3.62 | 3.8   | 1.21 | 184                    | 61.73  | 2.99  | 0.09   | 427              | 0.05 |
|                    |             | QT-10705   | 1                              | 0.1  | 1.24 | 1.34  | 1.26 | 124                    | 126    | 0.98  | 0.10   | 532              | 0.07 |
| 2                  |             | QT-2 10070 | 0.24                           | 0.05 | 0.98 | 1.03  | 0.13 | 408                    | 54.17  | 7.54  | 0.21   | 444              | 0.05 |
|                    |             | QT-2 12030 | 0.32                           | 0.1  | 0.99 | 1.09  | 0.38 | 309                    | 118.8  | 2.61  | 0.31   | 437              | 0.09 |
| 3                  |             | MOTA 2285  | 0.34                           | 0.02 | 0.21 | 0.23  | 1.22 | 62                     | 359    | 0.17  | 0.06   | 602              | 0.07 |
|                    |             | MOTA 2279  | 0.82                           | 0.03 | 0.6  | 0.63  | 1.08 | 73                     | 132    | 0.56  | 0.04   | 401              | 0.05 |
|                    |             | MOTA 2276  | 0.54                           | 0.05 | 0.31 | 0.36  | 0.94 | 57                     | 174    | 0.33  | 0.09   | 427              | 0.13 |
|                    |             | MOTA 2265  | 0.77                           | 0.08 | 0.44 | 0.52  | 1.26 | 57                     | 164    | 0.35  | 0.10   | 437              | 0.16 |
| 5                  |             | MOTA 2256  | 0.54                           | 0.02 | 0.22 | 0.24  | 1.18 | 41                     | 219    | 0.19  | 0.04   | 410              | 0.08 |
|                    |             | HZ 3741    | 0.61                           | 0.01 | 0.31 | 0.32  | 0.03 | 51                     | 5      | 10.33 | 0.02   | 430              | 0.02 |
|                    |             | HZ 3725    | 0.14                           | 0.01 | 0.35 | 0.36  | 0.24 | 250                    | 171    | 1.46  | 0.07   | 395              | 0.02 |
|                    |             | Jasa 87 G  | 0.29                           | 0.18 | 0.12 | 0.3   | 0.27 | 41.38                  | 93.1   | 0.44  | 0.62   | 435              | 0.6  |
| 6                  |             | Jasa 86 G  | 1.55                           | 1.52 | 2.97 | 4.49  | 0.67 | 191.61                 | 43.23  | 4.43  | 0.98   | 440              | 0.34 |
|                    |             | NAEF 3106  | 0.23                           | 0.03 | 0.11 | 0.14  | 1.39 | 48                     | 604    | 0.08  | 0.13   | 444              | 0.2  |
| 7                  | Sarcheshmeh | MEMO 1062  | 0.28                           | 0    | 0.1  | 0.1   | 0.7  | 36                     | 250    | 0.14  | 0.00   | 470              | 0.01 |
|                    |             | MEMO 998   | 0.2                            | 0    | 0.1  | 0.1   | 0.38 | 50                     | 190    | 0.26  | 0.00   | 406              | 0.02 |
|                    |             | MEMO 883   | 0.23                           | 0.01 | 0.14 | 0.15  | 0.28 | 61                     | 122    | 0.50  | 0.04   | 402              | 0.08 |
|                    |             | MEMO 857   | 0.21                           | 0.01 | 0.11 | 0.12  | 0.26 | 52                     | 124    | 0.42  | 0.05   | 403              | 0.05 |
|                    |             | MEMO 742   | 0.36                           | 0.01 | 0.13 | 0.14  | 0.37 | 36                     | 103    | 0.35  | 0.03   | 443              | 0.04 |
|                    |             | 5010 MAL   | 0.32                           | 0.01 | 0.34 | 0.35  | 0.38 | 106                    | 119    | 0.89  | 0.03   | 399              | 0.02 |
|                    |             | 4809 MAL   | 0.16                           | 0    | 0.42 | 0.42  | 0.2  | 262                    | 125    | 2.10  | 0.00   | 414              | 0.01 |
|                    |             | 4767 MAL   | 0.18                           | 0.01 | 0.21 | 0.22  | 0.22 | 117                    | 122    | 0.95  | 0.06   | 398              | 0.06 |
|                    |             | 4667 MAL   | 0.21                           | 0.06 | 0.11 | 0.17  | 0.13 | 52                     | 62     | 0.85  | 0.29   | 405              | 0.36 |
|                    |             | MAL 6606   | 0.47                           | 0.02 | 0.24 | 0.26  | 0.51 | 51                     | 109    | 0.47  | 0.04   | 443              | 0.07 |
| 8                  |             | MAL 6130   | 0.33                           | 0.04 | 0.2  | 0.24  | 0.37 | 61                     | 112    | 0.54  | 0.12   | 440              | 0.17 |
| 9                  |             | MOTA 1656  | 0.3                            | 0.01 | 0.37 | 0.38  | 0.18 | 123                    | 60     | 2.06  | 0.03   | 395              | 0.02 |
| 13                 |             | M 73       | 0.22                           | 0.07 | 0.22 | 0.29  | *    | 101                    | *      | *     | 0.32   | 443              | 0.24 |
|                    |             | M 69       | 0.24                           | 0.07 | 0.3  | 0.37  | *    | 125                    | *      | *     | 0.29   | 488              | 0.19 |
|                    |             | M 45       | 0.2                            | 0.08 | 0.22 | 0.3   | *    | 110                    | *      | *     | 0.40   | 475              | 0.27 |
|                    |             | M 42       | 0.19                           | 0.09 | 0.19 | 0.28  | *    | 102                    | *      | *     | 0.47   | 488              | 0.32 |
| 14                 |             | TS-1 2882  | 0.48                           | 0.1  | 0.52 | 0.62  | 2.53 | 108                    | 527    | 0.21  | 0.21   | 379              | 0.16 |
|                    |             | TS-1 2890  | 0.56                           | 0.11 | 0.53 | 0.64  | 1.32 | 95                     | 236    | 0.4   | 0.20   | 412              | 0.17 |
|                    |             | TS-1 2900  | 0.53                           | 0.12 | 0.49 | 0.61  | 1.5  | 92                     | 283    | 0.33  | 0.23   | 406              | 0.2  |
| Averages           |             |            | 0.68                           | 0.13 | 1.82 | 1.96  | 0.72 | 133.92                 | 158.42 | 3.05  | 0.17   | 434.66           | 0.13 |
| Standard deviation |             |            | 1.03                           | 0.30 | 5.57 | 5.75  | 0.57 | 128.97                 | 134.81 | 6.58  | 0.20   | 43.08            | 0.13 |
| 3                  | Sanganeh    | MOTA 2351  | 0.43                           | 0    | 0.28 | 0.28  | 1.24 | 65                     | 288    | 0.23  | 0.00   | 468              | 0.02 |
|                    |             | MOTA 2345  | 0.5                            | 0.01 | 0.33 | 0.34  | 1.24 | 66                     | 248    | 0.27  | 0.02   | 417              | 0.02 |
|                    |             | MOTA 2342  | 0.5                            | 0.01 | 0.29 | 0.3   | 1.14 | 58                     | 288    | 0.25  | 0.02   | 422              | 0.02 |
|                    |             | MOTA 2325  | 0.59                           | 0    | 0.23 | 0.23  | 1.18 | 39                     | 200    | 0.19  | 0.00   | 426              | 0.02 |
|                    |             | MOTA 2319  | 0.64                           | 0.01 | 0.26 | 0.27  | 1.73 | 41                     | 270    | 0.15  | 0.02   | 440              | 0.03 |
|                    |             | MOTA 2313  | 0.32                           | 0    | 0.16 | 0.16  | 1.06 | 50                     | 331    | 0.15  | 0.00   | 417              | 0.01 |
|                    |             | MOTA 2304  | 0.6                            | 0.02 | 0.25 | 0.27  | 1.19 | 42                     | 198    | 0.21  | 0.03   | 439              | 0.06 |
|                    |             | MOTA 2293  | 0.49                           | 0.01 | 0.31 | 0.32  | 1.22 | 63                     | 249    | 0.25  | 0.02   | 418              | 0.03 |
|                    |             | NAEF 1634  | 0.43                           | 0.02 | 0.22 | 0.24  | 0.15 | 51                     | 35     | 1.47  | 0.05   | 382              | 0.1  |
|                    |             | NAEF 1820  | 0.36                           | 0.01 | 0.69 | 0.7   | 0.9  | 192                    | 250    | 0.77  | 0.03   | 398              | 0.01 |
|                    |             | Jasa 89 G  | 0.32                           | 0.11 | 0.15 | 0.26  | 0.29 | 46.9                   | 90.6   | 0.52  | 0.34   | 437              | 0.42 |
|                    |             | Jasa 88 G  | 0.43                           | 0.3  | 0.29 | 0.59  | 0.19 | 67.5                   | 44.2   | 1.53  | 0.70   | 442              | 0.51 |
|                    |             | HZ 4266    | 0.47                           | 0.01 | 0.26 | 0.27  | 0.47 | 55                     | 100    | 0.55  | 0.02   | 439              | 0.03 |
|                    |             | HZ 4065    | 0.49                           | 0.01 | 0.35 | 0.36  | 0.42 | 71                     | 86     | 0.83  | 0.02   | 436              | 0.02 |
| HZ 4057            | 0.26        | 0          | 0.31                           | 0.31 | 0.32 | 119   | 123  | 0.97                   | 0.00   | 409   | 0      |                  |      |
| 6                  |             | MAL 5603   | 0.28                           | 0    | 0.14 | 0.14  | 0.49 | 50                     | 175    | 0.29  | 0.00   | 399              | 0    |
|                    |             | MAL 5722   | 0.42                           | 0.01 | 0.28 | 0.29  | 0.17 | 67                     | 40     | 1.65  | 0.02   | 393              | 0.03 |
|                    |             | MAL 5731   | 0.31                           | 0.03 | 0.15 | 0.18  | 0.31 | 48                     | 100    | 0.48  | 0.10   | 378              | 0.14 |
| 9                  |             | MAL 6130   | 0.33                           | 0.04 | 0.2  | 0.24  | 0.37 | 61                     | 112    | 0.54  | 0.12   | 440              | 0.17 |
| 10                 |             | MAL 6993   | 0.48                           | 0    | 0.19 | 0.19  | 0.38 | 40                     | 79     | 0.50  | 0.00   | 399              | 0.02 |
| 14                 |             | TS-1 2552  | 0.89                           | 0.36 | 1.11 | 1.47  | 1.39 | 125                    | 156    | 0.80  | 0.40   | 428              | 0.24 |
|                    |             | TS-1 2608  | 0.79                           | 0.37 | 1.35 | 1.72  | 1.71 | 171                    | 216    | 0.79  | 0.47   | 430              | 0.22 |
|                    |             | TS-1 2632  | 0.58                           | 0.4  | 1.5  | 1.9   | 1.84 | 259                    | 317    | 0.82  | 0.69   | 427              | 0.21 |
|                    |             | TS-1 2704  | 0.69                           | 0.31 | 1.12 | 1.43  | 1.78 | 162                    | 258    | 0.63  | 0.45   | 422              | 0.22 |
|                    |             | TS-1 2728  | 0.89                           | 0.28 | 0.98 | 1.26  | 1.71 | 110                    | 192    | 0.57  | 0.31   | 426              | 0.22 |
|                    |             | TS-1 2788  | 0.96                           | 0.2  | 0.8  | 1     | 1.63 | 83                     | 170    | 0.49  | 0.21   | 420              | 0.2  |
|                    |             | TS-1 2832  | 0.49                           | 0.09 | 0.58 | 0.67  | 2.42 | 118                    | 494    | 0.24  | 0.18   | 389              | 0.13 |
| TS-1 2840          | 0.44        | 0.08       | 0.48                           | 0.56 | 2.61 | 109   | 593  | 0.18                   | 0.18   | 381   | 0.14   |                  |      |
| Averages           |             |            | 0.51                           | 0.10 | 0.47 | 0.57  | 1.06 | 86.76                  | 203.67 | 0.58  | 0.16   | 418.64           | 0.12 |
| Standard deviation |             |            | 0.19                           | 0.14 | 0.39 | 0.51  | 0.70 | 53.97                  | 130.03 | 0.42  | 0.21   | 21.96            | 0.13 |

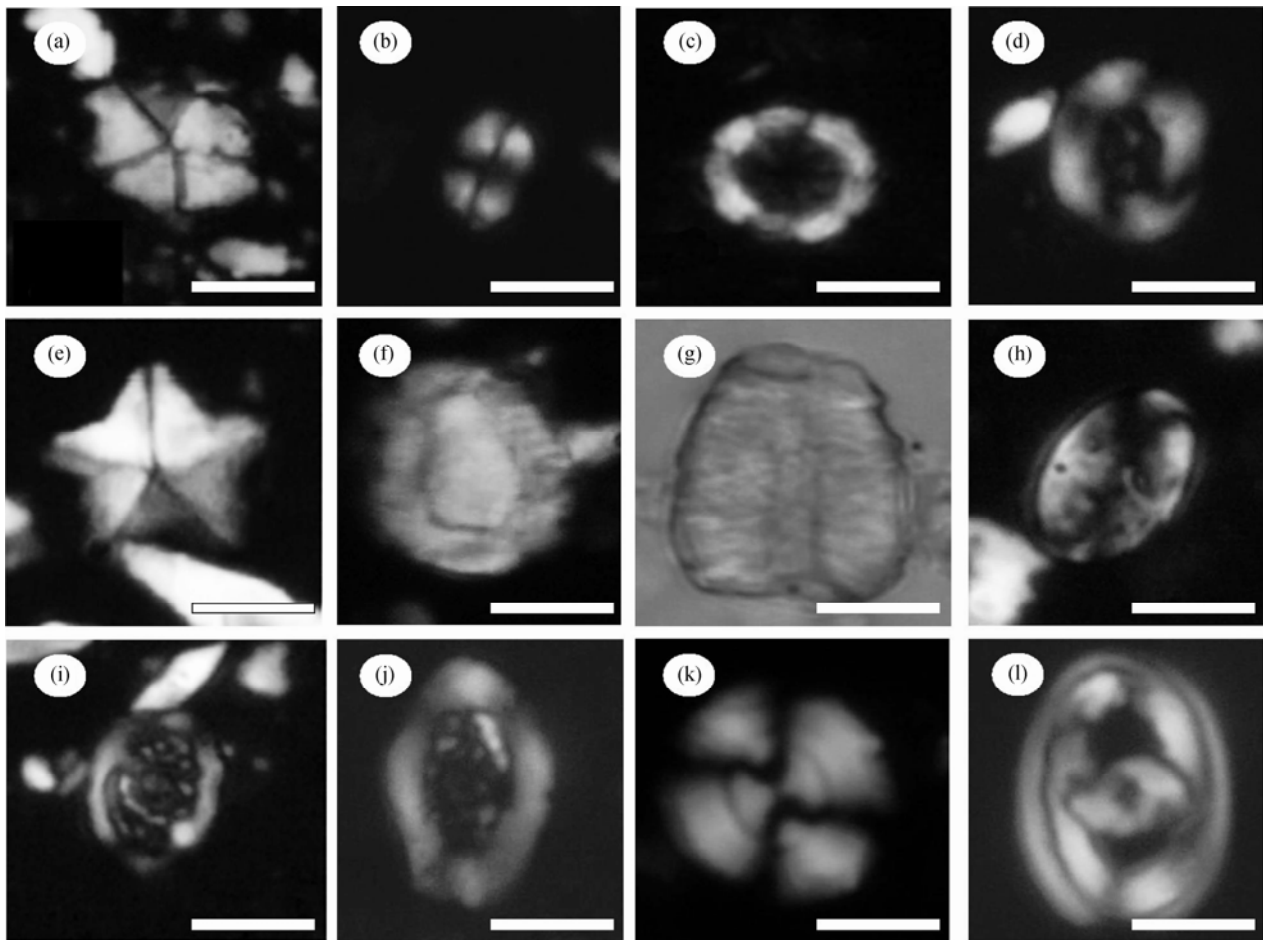


Fig. 3. Cross Polarized Light (XPL) and Plane Polarized Light (PPL) of calcareous nannofossil pictures from early Cretaceous of the Sarcheshmeh (=Sr.) and Sanghaneh (=Sn.) formations in the Qaleh-Zu and Qaleh-Jegh sections. Scale bars for all pictures represent 2  $\mu\text{m}$ .

(a) *Braarudosphaera hockwoldensis*, (XPL), Sample No. MAL 4837, Sr. Fm.; (b) *Calcutites percensis*, (XPL), Sample No. HZ 3204, Sn. Fm.; (c) *Eprolithus floralis*, (XPL), Sample No. MEMO 225, Sn. Fm.; (d) *Helenea chiestaia*, (XPL), Sample No. MEMO 904, Sr. Fm.; (e) *Micrantholithus obtusus*, (XPL), Sample No., MEMO 175, Sr. Fm.; (f) *Nannoconus bucheri*, (XPL), Sample No. MAL 4710, Sr. Fm.; (g) *Nannoconus steinmannii steinmannii*, (PPL), Sample No. MEMO 23, Sr. Fm.; (h) *Percivalia fenestrata*, (XPL), 45° rotated, Sample No. MEMO 205, Sr. Fm.; (i) *Rhagodiscus asper*, (XPL), Sample No. MEMO 180, Sr. Fm.; (j) *Rhagodiscus gallagheri*, (XPL), Sample No. MEMO 865, Sr. Fm.; (k) *Watznaueria biporta*, (XPL), Sample No. MAL 4892, Sr. Fm., (l) *Zeugrhabdotus embergeri*, (XPL), Sample No. MEMO 859, Sr. Fm.

Also, the partial parts of subzones CC7b –CC8a equivalent with partial parts of NC7-NC8 biozones were identified in the Sanganeh strata suggesting the age of Aptian-Albian for the formation. At the Qaleh-Zu section, it was not possible to retrieve all biozones and subzones due to the absence of some specific markers however, the CC7a and CC7b biozones of Sissingh, 1977 (NC6 and NC7 biozones of Roth, 1978) were detected within the Sarcheshmeh Formation though the marker species *Hayesites irregularis* for the base of the CC7a subzone was not identified. Therefore, an age of early Aptian is proposed to the Sarcheshmeh Fm. The recorded nannofossils from the Sanganeh Fm. do not allow their assignment to an exact geological age but, based on stratigraphic position, an age of late Aptian-Albian could be assigned to this rock unit. A severe decrease in nannoconoids abundance was detected in lower Aptian strata of the two sections that might be a signature for the

OAE1a interval that may need carbon isotope stratigraphy to confirm. This event has already been reported from the early Aptian strata in other parts of the Koppeh-Dagh basin (Mahanipour et al., 2011).

#### 4.2 Palynofacies, palaeoecology and palaeoenvironmental interpretations

Palynofacies analysis is a powerful tool for palaeoenvironmental interpretations and identification of petroleum source rocks (Al-Ameri et al., 2001; Obok-Ikuenobe and de Villiers, 2003; El Beialy et al., 2010; Silva et al., 2014; El Atfy et al., 2016). Palynofacies results can also be used alongside with biostratigraphic data in a sequence-stratigraphic framework in order to discover source rocks geometry. Palynological elements from all prepared slides were counted, grouped and percentages of the three main groups of kerogens were calculated. These are then plotted on the Tyson-type

diagram (Tyson, 1995) that resulted in recognition of seven palynofacies according to distance from the shoreline. The palynofacies are of types II, III, IV, V, VI, VII and IX, however types II, IV and VI are more dominant (Fig. 4). To increase the validity of the

depositional setting reconstruction, palaeoecology of the dinoflagellate cysts and coccolithophores are considered in interpretations. In the Qaleh-Zu section, the Sarcheshmeh Formation shows an alternation between palynofacies types II (marginal dysoxic basin) and IV (shelf to basin

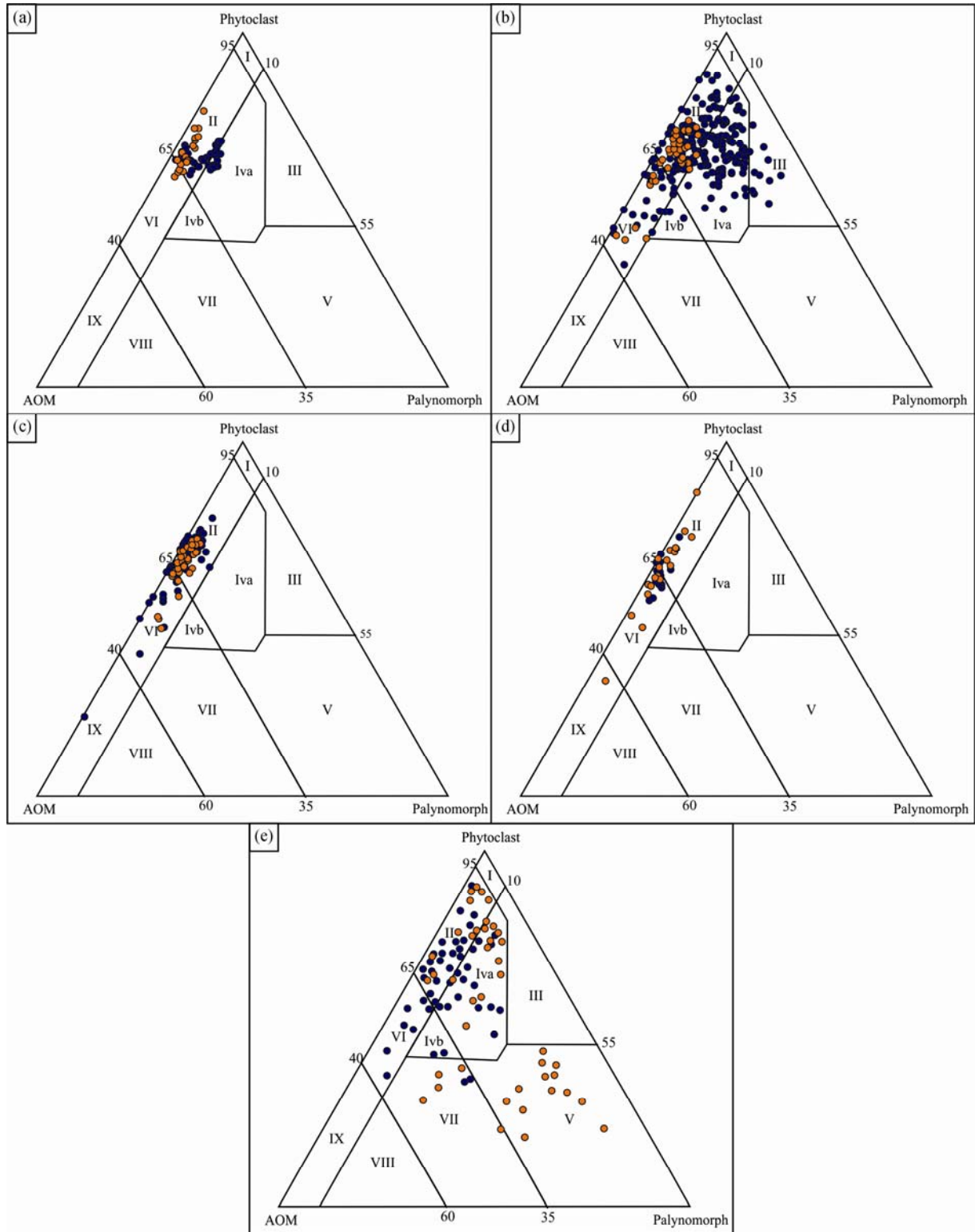


Fig. 4. Tyson-type diagrams (1995) for the Sarcheshmeh (blue circles) and Sanganeh (orange circles) formations. (a) Qaleh-Zu; (b) Qaleh-Jegh; (c) Boz-Dagh; (d) Taftazan; (e) Borehole A.

transition) but the Sanganeh Formation is dominant by palynofacies II. The studied successions at the Boz-Dagh and Taftazan sections display dominance of palynofacies types II and VI (proximal suboxic shelf) though the palynofacies IX (distal suboxic to anoxic basin) is rarely recorded in both sections. At the Qaleh-Jegh section, palaeoenvironmental studies revealed more varied range of palynofacies including II, III, IV and VI. However, similar to the Qaleh-Zu section, the Sanganeh strata are conquered by palynofacies type II of Tyson (1995). Most changes in palynofacies among the studied sections are recorded in the borehole A, where the palynofacies types II, IV, V, VI and VII are present. The palynofacies V and VII are belonging to the oxic and suboxic distal shelves respectively. Combination of these results make it possible to conclude a gradual sea level rise during the late Barremian to early Aptian and a marginal suboxic basin which was extended at the beginning of the Sarcheshmeh throughout the Koppeh-Dagh area that turned into a transitional zone between shelf and basin with a more diversified dinoflagellate cysts assemblage. This transgression is also proved by an increase in the number of chorate dinocyst forms (e.g. *Oligosphaeridium complex*) and decrease in *Muderongia* and *Subtilisphaera* genera towards the upper parts of the Sarcheshmeh Formation as suggested by Carvalho et al., 2006. Following, the sea level rise extended up into the Sanganeh Formation with some fluctuations. During the late Aptian to early Albian a marginal suboxic-anoxic basin was dominant in the western and central parts of the studied area but, towards the east, this environment locally changes to a distal oxic shelf (e.g. at the borehole A). Some additional palyno-palaeoecological parameters were also used here in order to uncover the palaeoenvironments' prevalent conditions. These include the ratios of brown to opaque phytoclasts (lability), light AOMs to dark AOMs, AOMs to brown phytoclasts, AOMs to marine palynomorphs, and finally, cubic to bladed phytoclasts. The calculated values for these ratios revealed a domination of a suboxic condition with low to medium sedimentation rates during depositional course of the formations (data presented as supplementary). These oxygen-depleted, low energy environments prepared unique conditions for preserving organic matter and deposition of source rocks (Demaison and Moore, 1980; Erbacher et al., 2001). However, the basal parts of the Sarcheshmeh Formation show slightly higher amounts of oxygen and also more oxic condition was recorded at the top of the Sanganeh Formation in the borehole A in the eastern part of the studied area. In addition, the numerous presence of warm water taxa such as *Rhagodiscus asper*, nannoconoids and pentolith group (e.g. *Micrantholithus hoschulzii*, *Micrantholithus obtusus* and *Braarudosphaera hockwoldensis*) and the absence of cool water taxa (*Repagulum* and *Crucibiscutum* genera) among the nannoflora communities, confirm the Tethyan realm warm waters (Mutterlose and Kessels, 2000; Street and Bown, 2000; Hardas and Mutterlose, 2007).

#### 4.3 Evaluation of petroleum potential

The Tethyan Basin experienced a period of organic-rich

sedimentation during the Early Aptian time known as the oceanic anoxic event 1a (OAE 1a) (Leckie et al., 2002; Steuber et al., 2005; Malinverno et al., 2010) that led to the deposition of high petroleum potential zones through the basin (Coccioni et al., 2006; Föllmi, 2012). This event is synchronous with the deposition of the rock units being studied here which are reported to be potentially petroleum source rocks in some parts of the basin (Kavoosi et al., 2010). Therefore, an integration of palynofacies analysis and Rock-Eval data is in use to evaluate their potential of hydrocarbon production and preservation. The relationship between organic elements remained in palynological slides and hydrocarbon generation is broadly studied (Batten and Stead, 2005; Zobaa et al., 2011). Generally, values of TOC in the Rock-Eval pyrolysis are in direct relation with the amount of AOMs in palynofacies studies (Jasper et al., 2010; Zobaa et al., 2011) as the AOM-rich zones are characteristic of type I oil-prone Kerogen. Kerogens types II and III are controlled by both AOMs and phytoclasts that indicate oil-to gas-prone horizons (Tyson, 1995). In the studied formations here, phytoclasts which are basic elements forming the gas-prone kerogen type III were mainly dominant.

Rock-Eval pyrolysis being based on the steady heating, is a rapid and inexpensive form of bulk analysis and now being used as a conventional method for evaluation of petroleum potential and generation of the various rock units (Behar et al., 2001; Baudin et al., 2015; Shekarifard, 2015; El Diasty et al., 2017) especially, for organic-rich fine-grained rocks that may play both source and/or reservoir roles for unconventional hydrocarbon systems (Jarvie, 2012; Gross et al., 2015). Estimation of amount of total organic carbon, thermal maturity degree and type of kerogens are main purposes for assessing source rock evaluation that are determined via the Rock-Eval pyrolysis (Bordenave et al., 1993; Alaug et al., 2013). As a results of Rock-Eval pyrolysis, the total organic carbon (TOC), maximum temperature ( $T_{max}$ ),  $S_1$ ,  $S_2$  and  $S_3$  parameters were measured and hydrogen index (HI), oxygen index (OI) and production index (PI) were calculated. To evaluate the hydrocarbon generation potential of the formations under study, Rock-Eval data from 63 rock samples available at the NIOC (Table 2) were used for interpretations. Based on these data, the measured TOC content in the studied successions usually are less than 1% however, the mean values are 0.68 and 0.51 wt% for the Sarcheshmeh and Sanganeh formations respectively proposing that these strata could act as a fair source rocks in some localities. For the Sarcheshmeh Formation  $T_{max}$  values fluctuate in a wide range from 379 to 602°C with an average of 435°C but, mostly were in range of 395 to 488°C, and varied from 378 to 468°C (frequently from 393 to 442°C) with an average of 419°C for the Sanganeh Fm. The  $T_{max}$  results in general show that the two formations under study are for their most parts in their immature stages except for a few samples which are placed in the early mature stage. To confirm these results, the spore coloration index (SCI) is evaluated and brought into consideration. The SCI is a maturation indicator that measures the color changes of palynomorphs, especially

spores and pollen grains in a scale of one to ten reflecting color gradation from yellow to black (Marshall, 1990; Utting and Hamblin, 1991) and as a function of estimating palaeo-temperatures and maturity levels. Based on this method, at the transition from the immature to early mature stages, yellow and light orange colors fades out while, dark orange and brown colors are supposed to appear. Our measure of palynomorphs maturity obtained via observing the color changes of spores and pollen grains in transmitted light (Fig. 5) is implemented. As a result, the majority of palynomorph grains reflected a color range from golden yellow (SCI 4) to dark brown (SCI 8) which is close to the thermal alteration index (TAI) 2–3 corresponding to the late immature–early hydrocarbon (oil and gas) generation zones. According to the literature (e.g., Espitalié et al., 1977; Tissot and Welte, 1984; Peters et al., 2005), the boundary between immature and early maturation stages is 435°C while, the maximum temperatures recorded here are mostly lower than this boundary. Unlike this, the spore coloration index shows that both formations experienced at least early maturation stages in the most parts of their stratigraphic columns that proved some discrepancies in the gained values of  $T_{max}$  parameter from the Rock-Eval pyrolysis.

The amount of free hydrocarbon ( $S_1$ ), ranged from 0 to

1.52 mg HC/g rock with an average of 0.13 for the Sarcheshmeh Formation and from 0 to 0.4 mg HC/g rock with an average of 0.1 for the Sanganeh Formation. The values for the  $S_2$  parameter oscillate between 0.1 and 29 mg HC/g rock with the mean value of 1.82 (the standard deviation is 5.57) for the Sarcheshmeh and from 0.14 to 1.5 for the Sanganeh Formation with an average of 0.47. According to the performed Rock-Eval analyses, the hydrocarbon potential ( $S_1+S_2$ ) of the Sarcheshmeh and Sanganeh formations ranges from 0.1 to 29.89 mg HC/g rock (the average values is 1.96) and 0.14 to 1.9 mg HC/g rock with an average of 0.57, respectively. The cross-plot of hydrocarbon potential versus TOC (Fig. 6a) for both formations indicates a mainly poor source rocks. The production index (PI) values of the hydrocarbon generation stage normally fluctuate between 0.1 to 0.4 (Tissot and Welte, 1984). This parameter varies from 0.01 to 0.6 with an average of 0.13 for Sarcheshmeh and from 0 to 0.51 for the Sanganeh with an average of 0.12 showing that both formations are positioned into the immature to early maturation stages. Peters and Cassa (1994) proposed that kerogen type of the source rocks could be determined via using  $S_2/S_3$  ratio. This ratio was calculated for the Sarcheshmeh and Sanganeh formations and with exception of three samples belonging to the Sarcheshmeh Formation,

| Boz-Dagh    |      |                   | Qaleh-Jegh  |      |                   | Taftazan    |     |                   | Qaleh-Zu    |      |                   | Borehole A  |      |                   |
|-------------|------|-------------------|-------------|------|-------------------|-------------|-----|-------------------|-------------|------|-------------------|-------------|------|-------------------|
| Fm.         | Tk.  | Spores and Pollen | Fm.         | Tk.  | Spores and Pollen | Fm.         | Tk. | Spores and Pollen | Fm.         | Tk.  | Spores and Pollen | Fm.         | Tk.  | Spores and Pollen |
| Sanganeh    | 1795 |                   | Sanganeh    | 3850 |                   | Sanganeh    | 684 |                   | Sanganeh    | 1253 |                   | Sanganeh    | 2496 |                   |
|             | 1734 |                   |             | 3344 |                   |             | 672 |                   |             | 1138 |                   |             | 2656 |                   |
|             | 1727 |                   |             | 2662 |                   |             | 666 |                   |             | 895  |                   |             | 2704 |                   |
|             | 1681 |                   |             | 2423 |                   |             | 638 |                   |             | 725  |                   |             | 2784 |                   |
|             | 1643 |                   |             | 1922 |                   |             | 577 |                   |             | 640  |                   |             | 2824 |                   |
| Sarcheshmeh | 1171 |                   | Sarcheshmeh | 1371 |                   | Sarcheshmeh | 348 |                   | Sarcheshmeh | 568  |                   | Sarcheshmeh | 2854 |                   |
|             | 966  |                   |             | 1010 |                   |             | 519 |                   |             | 2908 |                   |             |      |                   |
|             | 640  |                   |             | 525  |                   |             | 307 |                   |             | 2964 |                   |             |      |                   |
|             | 124  |                   |             | 155  |                   |             | 103 |                   |             | 45   |                   |             | 3004 |                   |

Fig. 5. Spore Color Index (SCI) for spores and pollen grains in the Sarcheshmeh and Sanganeh formations. Thickness (Tk.) and depth (Dp.) are in meters.

the values were below five that suggest kerogen types III (gas-prone kerogen) and IV (died kerogen). Furthermore, the cross-plots of S<sub>2</sub> and TOC (Fig. 6b) confirmed this and indicated presence of mainly kerogen type III through the studied formations. The hydrogen index (HI) is

another calculated parameter which is used to determine the type of kerogens. The HI value was between 36 and 544.2 mg HC/g TOC for the Sarcheshmeh (the mean value is 133.9) and 39 to 259 mg HC/g TOC (the average is 86.76) for the Sanganeh Fm. These low to moderate

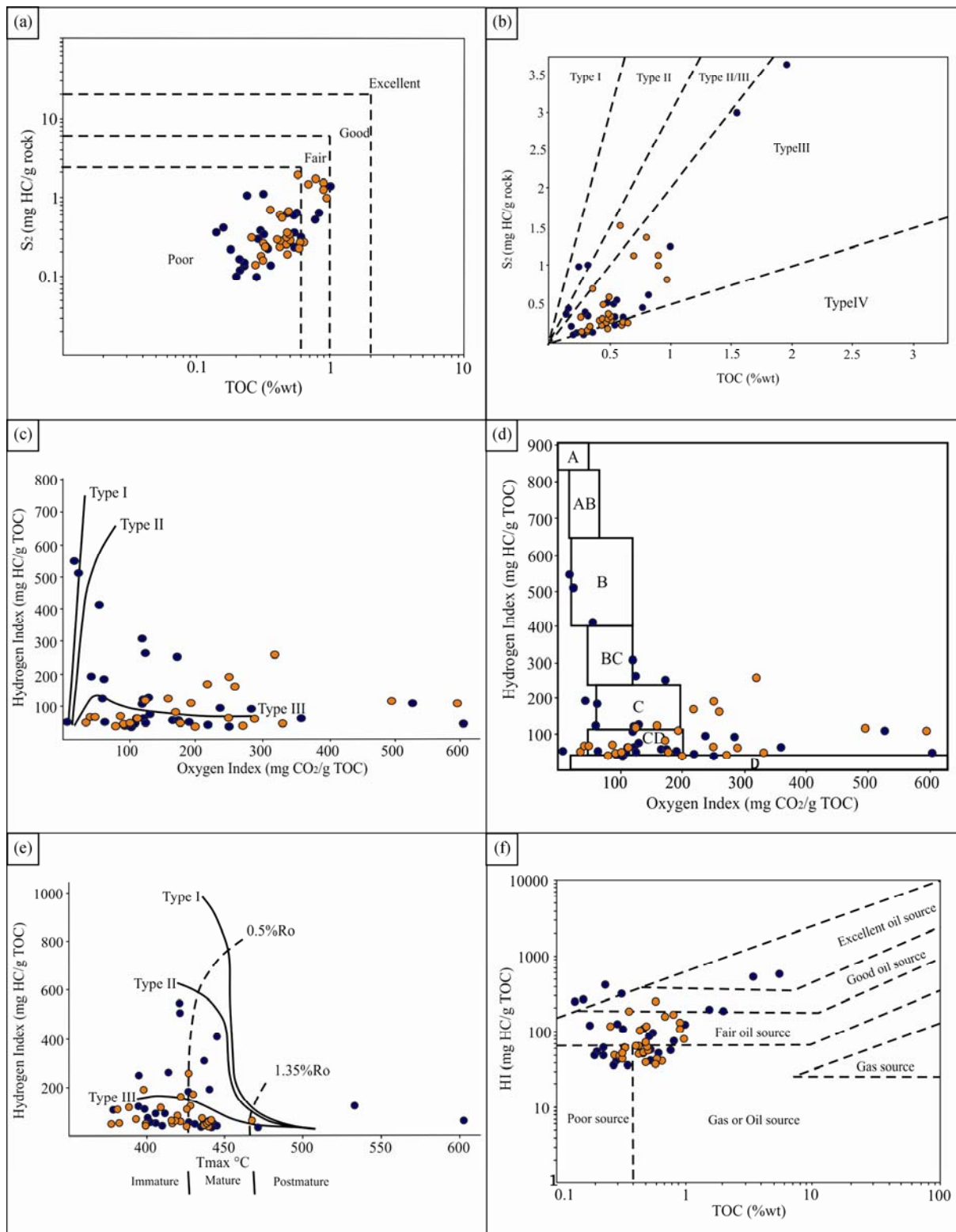


Fig. 6. Cross-plots of parameters gained from Rock-Eval pyrolysis. Blue dots: Sarcheshmeh Fm., Orange dots: Sanganeh Fm.

hydrogen indices show predominantly gas-prone kerogens (Boyer et al., 2006). The modified van-Krevelen diagram (HI versus OI cross-plot) of the Sarcheshmeh and Sanganeh samples (Fig. 6c) denotes presence of the kerogen types III and IV. Changes in the ratio of HI versus OI have also been utilized for determination of the organic facies. This ratio (Fig. 6d) suggested C and CD organic facies which are low oxygen environments with average sedimentation speed next to orogenic localities. Based on palynofacies investigations of Sarcheshmeh and Sanganeh formations, these organic facies are approximately equivalent to palynofacies type II and they are appropriate for sedimentation of gas-prone source rocks. The HI versus  $T_{max}$  diagram usually used for determination of

kerogen type and maturity of organic carbon content (Hunt, 1996) shows that the both formations are located mainly into the type III and IV kerogen areas (Fig. 6e) with immature to early maturation organic materials. The plot of HI versus TOC (Fig. 6f) revealed a poor barren to a gas-prone source rock for the both formations. An integration of these results shows that a big portion of the kerogen content is of the type III (phytoclads group) that confirmed by palynofacies investigations too (Fig. 7). The kerogen type III is mainly consists of humic coaly material derived from continental higher plants (phytoclads) that during the early stage of maturity can generate natural gas. This type of kerogen has low values of hydrogen and high values of oxygen indices and because of this it is a gas-

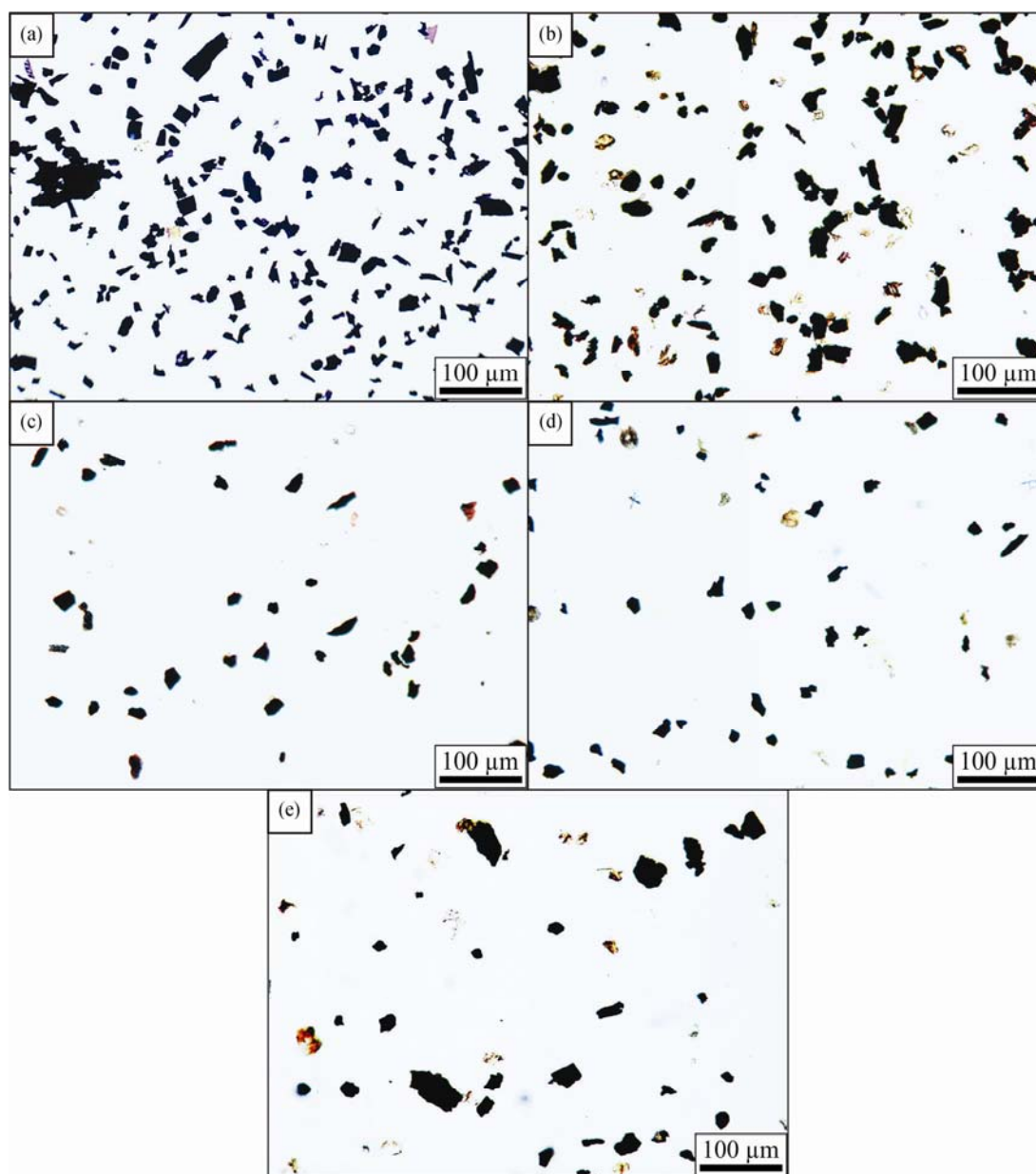


Fig. 7. Microphotographs of palynofacies II from the Sarcheshmeh and Sanganeh formations of the studied sections that reveal a large portion of the kerogen content is formed by the phytoclads group (kerogen type III). (a) Qaleh-Zu (Sample No. MEMO 225); (b) Qaleh-Jegh (Sample No. HZ 3206); (c) Boz-Dagh (Sample No. HZ 3927); (d) Taftazan (Sample No. MOTA 1703); (e) Borehole A (Sample No. 2870).

prone kerogen (Tissot and Walte, 1984). Although the low HI values is a reflection of large amounts of opaque phytoclasts but, generally the occurrences of low HI and TOC values alongside with thermally matured type III kerogen (that obtained via SCI observations) suggested natural gas generation during the past geological time. An interpretation to explain the discrepancy is that due to the maturation and generation, the organic matter content reduced eventually led to the low recorded values of TOC (Montgomery et al., 2005; Jarvie et al., 2007; Stein, 2007) and kerogen type III turned into type IV. These processes caused increase in relative frequency of residual bitumens which resulted records of some abnormalities in the Rock-Eval data. For example, the obtained maturity from the  $T_{max}$  and PI parameters are less than the maturity levels that gained from SCI observations. However, due to the lack of a good reservoir rock unit during the Late Cretaceous and Cenozoic a reservoir was not formed in the Koppeh-Dagh Basin in comparison with the synchronous deposits of the neighboring basins.

## 5 Conclusions

An integrated biostratigraphy, palynofacies, palaeoecology and Rock-Eval pyrolysis study performed on the Sarcheshmeh and Sanganeh formations in the Koppeh-Dagh Basin of northeastern Iran. Based on the recovered dinoflagellate cysts and calcareous nannofossils, an age of late Barremian-early Aptian was assigned to the Sarcheshmeh and Aptian-Albian to the Sanganeh Formation. Nannofossil investigations led to recognition of the CC7a-CC7b-CC8a nannozone of Sissingh (1977) and their equivalents (NC6-NC7-NC8) in Roth (1978) scheme. Palynological contents of the samples enabled us to define only a local palynozone, the *Odontochitina operculata* assemblage zone, with an age of late Barremian to Albian encompassing both formations. Quantitative palynofacies and palaeoecological observations were also performed in order to reconstruct the palaeoenvironment and the prevailed condition. These emphasized dominances of phytoclasts, mainly between 55 to 75%. As a result, a marginal basin with dysoxic to anoxic condition with low sedimentation rates was proposed for the basal parts of the Sarcheshmeh Formation. This environment turned into a transitional zone between shelf and basin with a more diversified dinoflagellate cyst assemblage as the sea level gradually rised. The dysoxic-anoxic marginal basin was extended upwards during deposition of the Sanganeh Formation though, an oxic shelf was recorded in the upper interval of the formation in the eastern parts of the studied area. An integration of Rock-Eval pyrolysis and palynofacies analysis is used here for evaluation of generation potential of the successions. For this Rock-Eval data were used for interpretations. The data show low values for the TOC and HI and high values for the OI. Also the Rock-Eval pyrolysis show that the gas-prone kerogen type III is dominant throughout the Sarcheshmeh and Sanganeh formations confirming the results gained from palynofacies analysis. The spore coloration index (SCI)

was undertaken to assess the organic maturation level of the rock units. The SCI observations (SCI 4-8), indicate that the organic matter content experienced thermally mature stages. The low HI and TOC values alongside with thermally mature gas-prone kerogen may suggest generation and migration of natural gas at some localities in the geologic past.

## Acknowledgements

The authors express their sincere gratitude to the exploration directorate of the National Iranian Oil Company (NIOC) and the University of Tehran for their support. Three anonymous reviewers who read the manuscript carefully and gave comments that improved the quality of the paper are greatly thanked.

Manuscript received Oct. 28, 2018

accepted Jan. 7, 2019

associate EIC HAO Zizuo

edited by Jeff LISTON and FEI Hongcai

## References

- Afshar-Harb, A., 1994. Geology of Kopet Dagh (in Persian). In: Hushmandzadeh A. (ed.), Treatise on the Geology of Iran. Geological Survey of Iran, Tehran.
- Al-Ameri, T.K., Al-Najar, T.K., and Batten, D.J., 2001. Palynostratigraphy and palynofacies indications of depositional environments and source potential for hydrocarbons: the mid Cretaceous Nahr Umr and lower Maaddud formations, Iraq. *Cretaceous Research*, 22: 735–742.
- Alaug, A.S., Batten, D.J., and Ahmed, A.F., 2013. Organic geochemistry, palynofacies and petroleum potential of the Mukalla Formation (late Cretaceous), Block 16, eastern Yemen. *Marine and Petroleum Geology*, 46: 67–91.
- Allen, M.B., Vincent, S.J., Alsop, G.I., Ismail-zadeh, A., and Flecker, R., 2003. Late Cenozoic deformation in the South Caspian region: effects of a rigid basement block within a collision zone. *Tectonophysics*, 366: 223–239.
- Backhouse, J., 2006. Albian (Lower Cretaceous) Dinoflagellate cyst Biostratigraphy of the Lower Gearle siltstone, Southern Carnarvon Basin, Western Australia. *Palynology*, 30: 43–68.
- Batten, D.J., and Stead, D.T., 2005. Palynofacies analysis and its stratigraphic application. In: E.A.E. Koutsoukos (ed.), *Applied Stratigraphy*, Dordrecht, 203–226.
- Baudin, F., Disnar, J.R., Aboussou, A., and Savignac, F., 2015. Guidelines for Rock-Eval analysis of recent marine sediments. *Organic Geochemistry*, 86: 71–80.
- Behar, F., Beaumont, V., Penteado, H.L., and De, B., 2001. Rock-Eval 6 Technology: Performances and Developments Oil & Gas Science and Technology. Review of the French Petroleum Institute, 56 (2): 111–134.
- Bellanca, A., Erba, E., Neri, R., Premoli-Silva, I., Sprovieri, M., Tremolada, F., and Verga, D., 2002. Paleocyanographic significance of the Tethyan “Livello Selli” (Early Aptian) from the Hyblan Formation, northwestern Sicily: biostratigraphy and high-resolution chemostratigraphic records. *Palaeogeography, Palaeoclimatology, Palaeoecology*, 185: 175–196.
- Bice, K.L., Birgel, D., Meyers, P.A., Dahl, K.A., Hinriches, K.U., and Norris, R.D., 2006. A multiple proxy and model study of Cretaceous upper ocean temperatures and atmospheric CO<sub>2</sub> concentrations. *Paleoceanography*, 21, PA2002. Doi: 10.1029/2005PA001203.
- Bordenave, M.L., Espitalié, L., Leplat, P., Oudin, J.L., and Vandenbroucke, M., 1993. Screening techniques for source rock evaluation. In: M.L. Bordenave (ed.), *Applied Petroleum Geochemistry*. Editions Technip, Paris, 217–278.
- Bornemann, A., Norris, R.D., Friedrich, O., Beckmann, B.,

- Schouten, S., Sinninghe-Damste, J., Vogel, J., Hofmann, P., and Wagner, T., 2008. Isotopic evidence for glaciation during the Cretaceous super-greenhouse, *Science*, 319: 189–192. Doi: 10.1126/science.1148777.
- Bown, P.R., 1998. *Calcareous Nannofossil Biostratigraphy*. In: British Micropaleontology Society Publication Series. *Calcareous Nannofossil Biostratigraphy*. Chapman and Hall/Kluwer Academic Publisher, London, 328 pp.
- Boyer, C., Kieschnick, J.; Suarez-Rivera, R., Lewis, R., and Waters, G., 2006. Producing gas from its source. *Oil Field Review*, Autumn 2006, 36–49.
- Bralower, T.J., Sliter, W.V., Arthur, M.A., Leckie, R.M., Allard, D., and Schlanger, S.O., 1993. Dysoxic/anoxic episodes in the Aptian - Albian (Early Cretaceous). In: Pringle, M.S., Sager, W.W., Sliter, W.V., and Stein, S., (eds.), *The Mesozoic Pacific: Geology, Tectonics and Volcanism*, Geophysical Monograph, American Geophysical Union, 77: 5–37.
- Bralower, T.J., 1987. Valanginian to Aptian calcareous nannofossil stratigraphy and correlation with the upper M-sequence magnetic anomalies. *Marine Micropaleontology*, 11: 293–310.
- Carvalho, M.A., Filho, J.G.M., and Menezes, T.R., 2006. Palynofacies and sequence stratigraphy of the Aptian–Albian of the Sergipe Basin, Brazil. *Sedimentary Geology*, 192: 57–74.
- Coccioni, R., Luciani, V., and Marsili, A., 2006. Cretaceous oceanic anoxic events and radially elongated chambered planktonic foraminifera: paleoecological and paleoceanographic implications. *Palaeoceanography, Palaeoclimatology, Palaeoecology*, 235: 66–92.
- Demaison G.J., and Moore G.T., 1980. Anoxic environments and oil source bed genesis. *American Association of Petroleum Geologists Bulletin*, 64: 1179–1209.
- Dumitrescu, M., Brassell, S.C., Schouten, S., Hopmans, E.C., and Damsté, J.S.S., 2006. Instability in tropical Pacific sea-surface temperatures during the early Aptian. *Geology*, 34: 833–836.
- El Atfy, H., Abeed, Q., Uhl, D., and Littke, R., 2016. Palynology, palynofacies analysis, depositional environments and source rock potential of Lower Cretaceous successions in southern Iraq. *Marine and Petroleum Geology*, 76: 362–376.
- El Beialy, S.Y., El Atfy, H.S., Zavada, M.S., El Khoriby, E.M., and Abu-Zied, R.H., 2010. Palynological, palynofacies, paleoenvironmental and organic geochemical studies on the Upper Cretaceous succession of the GPTSW-7 well, North Western Desert, Egypt. *Marine and Petroleum Geology*, 27: 370–385.
- El Diasty, W.Sh., El Beialy, S.Y., Mostafa, A.R., El Adl, H.A., and Batten, D.J., 2017. Hydrocarbon source rock potential in the southwestern Gulf of Suez graben: Insights from organic geochemistry and palynofacies studies on samples from the Ras El Bahar Oilfield. *Marine and Petroleum Geology*, 80: 133–153.
- Erba, E., 2004. Calcareous nannofossils and Mesozoic oceanic anoxic events. *Marine Micropaleontology*, 52: 85–106.
- Erba, E., and Tremolada, F., 2004. Nannofossil carbonate fluxes during the Early Cretaceous: phytoplankton response to nutrification episodes, atmospheric CO<sub>2</sub> and anoxia. *Palaeoceanography*, 19: 1–18.
- Erba, E., Bottini, C., Weissert, J.H., and Keller, C.E., 2010. Calcareous nannoplankton response to surface-water acidification around oceanic anoxic event 1a. *Science*, 329: 428–432.
- Erbacher, J., Huber, B.T., Norris, R.D., and Markey, M., 2001. Increased thermohaline stratification as a possible cause for an oceanic anoxic event in the Cretaceous period. *Nature*, 409: 325–327.
- Espitalié, J., Laporte, J.L., Madec, M., Marquis, F., Leplat, P., Paulet, J., and Boutefeu, A., 1977. Méthode rapide de caractérisation des roches de mères de leur potentiel pétrolier et de leur degré d'évolution. *Institut Français Pétrolier Revue*, 32: 23–42.
- Föllmi, K.B., 2012. Early Cretaceous life, climate and anoxia. *Cretaceous Research*, 35: 230–257.
- Foroughi, F., Gardin, S., Lotfali-Kani, A., and Vahidinia, M., 2017. Calcareous nannofossil biostratigraphy of Campanian strata (Abtalkh Formation) from the eastern Koppeh-Dagh Basin, NE Iran. *Cretaceous Research*, 70: 55–70.
- Garzanti, E., and Gaetani, M., 2002. Unroofing history of Late Paleozoic magmatic arcs within the Turan Plate (Tuarkyr, Turkmenistan). *Sedimentary Geology*, 151: 67–87.
- Gard, G., Backhouse, J., and Crux, J., 2016. Calibration of Early Cretaceous dinoflagellate zones from the NWS of Australia to the global time scale through calcareous nannofossils. *Cretaceous Research*, 61: 180–187.
- Ghasemi-Nejad, E., Head, M.J., and Naderi, M., 2009. Palynology and petroleum potential of the Kazhdumi Formation (Cretaceous: Albian – Cenomanian) in the South Pars field, northern Persian Gulf. *Marine and Petroleum Geology*, 26: 805–816.
- Glennie, K.W., 2000. Cretaceous tectonic evolution of Arabia eastern plate margin: a tale of two oceans, in Middle East models of Jurassic/Cretaceous carbonate systems. *SEPM Special Publication*, 69: 9–20.
- Gross, D., Sachsenhofer, R.F., Bechtel, A., Pytlak, B., Rupprecht, B., and Wegerer, E., 2015. Organic geochemistry of Mississippian shales (Bowland Shale Formation) in central Britain: Implications for depositional environment, source rock and gas shale potential. *Marine and Petroleum Geology*, 59: 1–21.
- Hardas, P., and Mutterlose, J., 2007. Calcareous nannofossil assemblages of Oceanic Anoxic Event 2 in the equatorial Atlantic: evidence of an eutrophication event. *Marine Micropaleontology*, 66: 52–69.
- Helby, R., Morgan, R., and Partridge, A.D., 2004. Updated Jurassic and Early Cretaceous dinocyst zonation NWS Australia. *Geoscience Australia Publication*.
- Herrle, J.O., and Mutterlose, J., 2003. Calcareous nannofossils from the Aptian-Lower Albian of southeast France: palaeoecological and biostratigraphic implications. *Cretaceous Research*, 24: 1–22.
- Hunt, J.M., 1996. *Petroleum Geochemistry and Geology*, 2nd ed. W.H. Freeman and Company, New York, 743.
- Huber, B.T., Norris, R.D., and Macleod, K.G., 2002. Deep-sea paleotemperature record of extreme warmth during the Cretaceous. *Geology*, 30: 123–126.
- Jasper, K., Hartkopf-Fröder, C., Flajs, G., and Littke, R., 2010. Evolution of Pennsylvanian (Late Carboniferous) peat swamps of the Ruhr Basin, Germany: Comparison of palynological, coal petrographical and organic geochemical data. *International Journal of Coal Geology*, 83(4): 346–365.
- Jarvie, D.M., Hill, J.R., Ruble, T.E., and Pollastro, R.M., 2007. Unconventional shale-gas systems: the Mississippian Barnett Shale of north-central Texas as one model for thermogenic shale-gas assessment. *American Association of Petroleum Geologists Bulletin*, 91: 475–499.
- Jarvie, D.M., 2012. Shale resource systems for oil and gas: Part 1—Shale-gas resource systems, in J. A. Breyer, ed., *Shale reservoirs—Giant resources for the 21st century*. American Association of Petroleum Geologists Bulletin, 97: 69–87.
- Kavoosi, M.A., Daryabandeh, M., Jamali, A.M., Bagheriy-Tirtashi, R., Ebadian, H., and Sherhati, Sh., 2010. Unconventional shale gas reservoirs in Iran, NIOC, Exploration directorate, TR 1914.
- Keller, C.E., Hochuli, P.A., Weissert, H., Bernasconi, S.M., Giorgioni, M., and Garcia, T.I., 2011. A volcanically induced climate warming and floral change preceded the onset of OAE1a (Early Cretaceous). *Palaeogeography, Palaeoclimatology, Palaeoecology*, 305: 43–49.
- Leckie, R.M., Bralower, T.J., and Cashman, R., 2002. Oceanic anoxic events and plankton evolution: biotic response to tectonic forcing during the mid-Cretaceous. *Palaeoceanography*, 17: 13–29.
- Mahanipour, A., Mutterlose, J., Lotfali-Kani, A., and Adabi, M.H., 2011. Palaeoecology and biostratigraphy of early Cretaceous (Aptian) calcareous nannofossils and the  $\delta^{13}\text{C}$  Carbon isotope record from NE Iran. *Cretaceous Research*, 32: 331–356.
- Malinverno, A., Erba, E., and Herbert, T.D., 2010. Orbital tuning

- as an inverse problem: Chronology of the early Aptian oceanic anoxic event 1a (Selli Level) in the Cismon APTICORE. *Paleoceanography*, 25, PA2203, doi:10.1029/2009PA001769.
- Marshall, J.E.A., 1990. Determination of thermal maturity. In: Briggs, D.E.G., and Crowther, P. (eds.), *Palaeobiology – a synthesis*, 511–515. Blackwell Scientific Publications, Oxford, UK.
- Montgomery, S.L., Jarvie, D.M., Bowker, K.A., and Pollastro, R.M., 2005. Mississippian Barnett shale, Fort Worth Basin, north-central Texas: gas-shale play with multitrillion cubic foot potential. *American Association of Petroleum Geologists Bulletin*, 89: 155–175.
- Morgan, R., Hooker, N., and Ingram, B., 2002. Towards higher palynological resolution in the Australian Mesozoic. Morgan Palaeo & Associates Report, 10p. Unpublished.
- Mutterlose, J., and Kessels, K., 2000. Early Cretaceous calcareous nannofossils from the high latitudes: implications for palaeobiogeography and palaeoclimate. *Palaeogeography, Palaeoclimatology, Palaeoecology*, 160: 347–372.
- Norris, R.D., Bice, K.L., Magno, E.A., and Wilson, P.A., 2002. Jiggling the tropical thermostat in the Cretaceous hothouse. *Geology*, 30: 299–302.
- Oboh-Ikuenobe, F.E., and Sue, E. de Villiers, 2003. Dispersed organic matter in samples from the western continental shelf of Southern Africa: palynofacies assemblages and depositional environments of Late Cretaceous and younger sediments. *Palaeogeography, Palaeoclimatology, Palaeoecology*, 201: 67–88.
- Ooisting, A.M., Leereveld, H., Dickens, G.R., Henderson, R.A., and Brinkhuis, H., 2006. Correlation of Barremian-Aptian (Mid-Cretaceous) dinoflagellate cyst assemblages between the Tethyan and Austral realms. *Cretaceous Research*, 27: 792–813.
- Partridge, A.D., 2006. Australian Mesozoic and Cenozoic Palynology Zonations (Charts 1–4). In: Monteil, E. (coord.), *Australian Mesozoic Palynology Zonations - updated to the 2004 Geologic Time Scale*. Geoscience Australia Record 2006/23. ISBN 1 921 236 05 1.
- Perch-Nielsen, K., 1985. Mesozoic Calcareous Nannofossils. In: Bolli, H.M., Saunders, J.B., and Perch-Nielsen, K. (eds.), *Plankton Stratigraphy*, Cambridge Earth Science Series. Cambridge University Press, 329–426.
- Peters, K.E., and Cassa, M.R., 1994. Applied source rock geochemistry. *American Association of Petroleum Geologists Memoir*, 60: 93–120.
- Peters, K.E., Walters, C.C., and Moldowan, J.M., 2005. *The biomarker guide*, second ed. Prentice Hall, New Jersey.
- Quattrocchio, M.E., Martinez, M.A., Carpinelli, P.A., and Volkheimer, W., 2006. Early Cretaceous palynostratigraphy, palynofacies and palaeoenvironments of well sections in Northeastern Tierra del Fuego, Argentina. *Cretaceous Research*, 27: 584–602.
- Radmacher, W., Tyszka, J., Mangerud, G., and Pearce, M.A., 2014. Dinoflagellate cyst biostratigraphy of the Upper Albian to Lower Maastrichtian in the southwestern Barents Sea. *Marine and Petroleum Geology*, 57: 109–121.
- Robert, A.M.M., Letouzey, J., Kavooosi, M.A., Sherkat, Sh., Müller, C., Vergés, J., and Aghababaei, A., 2014. Structural evolution of the Kopeh-Dagh fold-and-thrust belt (NE Iran) and interactions with the South Caspian Sea Basin and Amu Darya Basin. *Marine and Petroleum Geology*, 57: 68–87.
- Roth, P.H., 1978. Cretaceous nannoplankton biostratigraphy and oceanography of the northwestern Atlantic Ocean. In: Benson, W.E., Sheridan, R.E., et al. (eds.), *Initial Reports DSDP, 44*. U.S. Govt. Printing Office, Washington, 731–759.
- Sharifi, M., Ghasemi-Nejad, E., Sarfi, M., Yazdi-Moghadam, M., Tarjani-Salehani, M., and Akhtari, M., 2018. Marine palynology and environmental interpretation of the lower Cretaceous (Barremian? – Aptian) rock units in Koppeh-Dagh Basin, NE Iran. *Geological Quarterly*, 62 (1): 90–99.
- Shekarifard, A., 2015. A new approach to interpreting relationship between Rock-Eval S<sub>2</sub> and TOC data for source rock evaluation based on regression analyses. *Geopersia*, 5(1): 1–6.
- Street, C., and Bown, P.R., 2000. Palaeobiogeography of Early Cretaceous (Berriasian–Barremian) calcareous nannoplankton. *Marine Micropaleontology*, 39: 265–291.
- Silva, R.L., Mendonça Filho, J.G., Azerêdo, A., and Duarte, L.V., 2014. Palynofacies and TOC analysis of marine and non-marine sediments across the Middle-Upper Jurassic boundary in the central-northern Lusitanian Basin (Portugal). *Facies*, 60: 255–276.
- Sissingh, W., 1977. Biostratigraphy of Calcareous Nannoplankton. *Geologie En Mijnbouw*, 56: 37–65.
- Steuber, T., Rauch, M., Masse, J.P., Graaf, J., and Malkoc, M., 2005. Low-latitude seasonality of Cretaceous temperatures in warm and cold episodes. *Nature*, 437: 1341–1344.
- Stein, R., 2007. Upper Cretaceous/lower Tertiary black shales near the North Pole: organic-carbon origin and source-rock potential. *Marine and Petroleum Geology*, 24: 67–73.
- Stover, L.E., Brinkhuis, H., Damassa, S.P., de Verteuil, L., Helby, R., Monteil, E., Partridge, A.D., Powell, A.J., Riding, I.B., Smelror, M., and Williams, G.L., 1996. Mesozoic-Tertiary Dinoflagellates, Acritarchs and Prasinophytes. *American Association of Stratigraphic Palynologists Foundation*, 2: 641–750.
- Tahoun, S.S., Deaf, A.S., and Led, I.B., 2018. The use of cyclic stratigraphic pattern of peridinioid and gonyaulacoid dinoflagellate cysts in differentiating potential thick monotonous carbonate reservoirs: A possible ecostratigraphic tool under test. *Marine and Petroleum Geology*, 96: 240–253.
- Tejada, M.L.G., Suzuki, K., Kuroda, J., Coccioni, R., Mahoney, J.J., Ohkouchi, N., Sakamoto, T., and Tatsumi, Y., 2009. Ontong Java Plateau eruption as a trigger for the early Aptian oceanic anoxic event. *Geology*, 37: 855–858.
- Tissot, B.P., and Welte, D.H., 1984. *Petroleum formation and occurrence*. Springer, New York.
- Torricelli, S., 2000. Lower Cretaceous dinoflagellate cyst and acritarch stratigraphy of the Cimón APTICORE (Southern Alps, Italy). *Review of Palaeobotany and Palynology*, 108: 213–266.
- Traverse, A., 2007. *Paleopalynology*. 2nd Edition, Springer.
- Tremolada, F., Erba, E., and Bralower, T.J., 2006. Late Barremian to early Aptian calcareous nannofossil paleoceanography and paleoecology from the Ocean Drilling Program Hole 641C (Galicia Margin). *Cretaceous Research*, 27: 887–897.
- Tremolada, F., and Erba, E., 2002. Morphometric analysis of the Aptian *Rucinolithus terebrodentarius* and *Assipetra infracretacea* nannoliths: Implications for taxonomy, biostratigraphy and paleoceanography. *Marine Micropaleontology*, 44: 77–92.
- Tyson, R.V., 1995. *Sedimentary Organic Matter, Organic Facies and Palynofacies*. Chapman and Hall, London.
- Ulmishek, G.F., and Klemme, H.D., 1990. Depositional controls, distribution, and effectiveness of world's petroleum source rocks. *US Geological Survey Bulletin*, Report # B, 1931, pp. 59.
- Utting, J., and Hamblin, A.P., 1991. Thermal maturity of the Lower Carboniferous Horten Group, Nova Scotia. *International Journal of Coal Geology*, 13: 439–456.
- Van-Breugel, Y., Schouten, S., Tsikos, H., Erba, E., Price, G.D., and Sinninghe-Damsté, J.S., 2007. Synchronous negative carbon isotope shifts in marine and terrestrial biomarkers at the onset of the early Aptian oceanic anoxic event 1a: Evidence for the release of <sup>13</sup>C-depleted carbon into the atmosphere. *Paleoceanography*, 22, PA1210, doi:10.1029/2006PA001341.
- Watkins, D.K., 2007. Quantitative analysis of the calcareous nannofossil assemblages from CIROS-1, Victoria Land Basin, Antarctica. *Journal of Nannoplankton Research*, 29 (2): 130–137.
- Zobaa, M.K., Oboh-Ikuenobe, F.E., and Ibrahim, M.I., 2011. The Cenomanian/Turonian oceanic anoxic event in the Razzak Field, north Western Desert, Egypt: Source rock potential and paleoenvironmental association. *Marine and Petroleum Geology*, 28 (8): 1475–1482.

**About the first author**

Sharifi MOHAMMAD is a marine palynologist with interest areas of palynology, sedimentary environment reconstructions and petroleum potential evaluation of source rock units. He received a BSc (2010) in Geology from Isfahan University, Iran and an MSc (2013) and a PhD (2019) in Stratigraphy and Paleontology from the University of Tehran, Iran.

**About the corresponding author**

Dr. Ghasemi-Nejad EBRAHIM did his Ph.D. at the Department of Earth Sciences of the University of Saskatchewan, Canada from 1990 to 1995 on Palynology and Palaeoenvironment of the Jurassic strata of the Jura Mountains in Switzerland. In 1996 he started working with the Department of Geology of the University of Tehran where he is now a professor teaching and handling research projects in the fields of Marine Palynology, and evaluation of petroleum potential of different rock units via using these characters and published many papers on these subjects. He is currently active and also acts as the chief editor of the Geopersia journal. [eghasemi@khayam.ut.ac.ir](mailto:eghasemi@khayam.ut.ac.ir)